Trajectory structures and transport

Madalina Vlad and Florin Spineanu
National Institute of Fusion Science, Toki 509-5292, Japan
and National Institute for Laser, Plasma and Radiation Physics, Association Euratom–MEC Romania, P.O. Box MG-36, Magurele, Bucharest, Romania
(Received 18 September 2003; revised manuscript received 28 April 2004; published 15 November 2004)

The special problem of transport in two-dimensional divergence-free stochastic velocity fields is studied by developing a statistical approach, the nested subensemble method. The nonlinear process of trapping determined by such fields generates trajectory structures whose statistical characteristics are determined. These structures strongly influence the transport.

DOI: 10.1103/PhysRevE.70.056304 PACS number(s): 47.27.Qb, 52.35.Ra, 05.40.−a, 05.10.Gg

I. INTRODUCTION

Test particle motion in stochastic velocity fields (or tracer advection) is a generic problem in various topics of fluid and plasma turbulence, astrophysics, or solid state physics [1–5]. This problem is strongly related to the process of advection-diffusion of passive and active fields, which was very much studied in recent years, and important progress was achieved [6–9].

In this context, particle motion in two-dimensional divergence-free velocity fields represents a special case. Kraichnan has shown, for the first time, in a study based on numerical simulations [10], that the existing analytical methods are not adequate for this type of problem. The cause of this anomaly is the trapping of the particles, which appears in such velocity fields when they have slow time variation. The trapping consists in trajectory winding on almost closed paths. A typical trajectory has a complicated shape with such localized trapping events separated by long jumps. Consequently, the probability distribution function is non-Gaussian. Thus the methods based on this hypothesis (like that of Corrsin [11,1] and the direct interaction approximation [10,12,13]) are not adequate for this specific case.

This special problem of diffusion in two-dimensional divergence-free velocity fields describes, for instance, the transport in turbulent magnetized plasmas or in incompressible fluids. It was studied especially by means of direct numerical simulations ([14] and the references therein) or on the basis of simplified models [15,16]. There is also a qualitative theoretical estimation of the scale law for the asymptotic diffusion coefficient [17] based on an analogy with the percolation process in stochastic landscapes. The case of collisional particle motion in such static velocity fields was analyzed by means of renormalization group techniques ([2] and the references therein) and the asymptotic time behavior of the mean square displacement was determined. The evolution of the diffusion process of test particles was determined only in [18] where a statistical approach, the decorrelation trajectory method, was developed. It yields analytical expressions for the time-dependent diffusion coefficient $D(t)$ and for the correlation of the Lagrangian velocity $L(t)$ that are qualitatively valid for the whole range of the Kubo number (see the next section for the definitions). This method could be extended to more complicated physical systems which contain particle collisions, average velocities, or a supplementary component of the motion perpendicular to the two-dimensional plane ([19] and the references therein). It was shown that the presence of trapping determines memory effects in $L(t)$ and a rich class of anomalous diffusion regimes in the presence of a decorrelation mechanism [19]. These studies have shown that the decorrelation trajectory method provides a qualitatively good description of the trapping process. However, due to the rather strong approximation introduced in this method (see Sec. III), there are several qualitative aspects that are not well described [20,21]. They are related to trajectory fluctuations and their correlation with the stochastic velocity.

The above results concern the effect of trapping on the individual trajectories. We show here that trapping also produces collective effects. It determines coherence in the stochastic motion in the sense that bundles of neighboring trajectories form localized structures similar to fluid vortices. The statistical characteristics of trapped and free trajectories are separately studied and the average, the dispersion, and the probability distribution, function for the trajectories and for the distance between two neighboring trajectories are determined.

The method developed for this study, the nested subensemble method, is a semianalytical statistical approach which extends and improves the decorrelation trajectory method [18] by taking into account the fluctuations of the trajectories in the subensembles. This is a Lagrangian method constructed with the aim of being in agreement with the statistical constraints imposed by the conservation of the Lagrangian potential in each realization. We note that our method is completely different from the recent Lagrangian approaches based on statistical conservation laws (see the review [6]).

II. THE PROBLEM

Particle advection in a two-dimensional stochastic velocity field is described by the nonlinear Langevin equation

$$\frac{d\mathbf{x}(t)}{dt} = \mathbf{v}[\mathbf{x}(t),t], \quad \mathbf{x}(0) = \mathbf{0}, \tag{1}$$

where $\mathbf{x}(t)$ represents the trajectory in Cartesian coordinates $\mathbf{x} \equiv (x_1, x_2)$ The stochastic velocity field $\mathbf{v}(\mathbf{x},t)$ is divergence-

free: $\nabla \cdot \mathbf{v}(\mathbf{x},t)=0$, and thus its two components v_1 and v_2 can be determined from the stochastic scalar field $\phi(\mathbf{x},t)$ as

$$v_i(\mathbf{x},t) = \varepsilon_{ij}\frac{\partial \phi(\mathbf{x},t)}{\partial x_j} \tag{2}$$

where ε_{ij} is an antisymmetric tensor ($\varepsilon_{12}=1$, $\varepsilon_{21}=-1$, $\varepsilon_{11}=\varepsilon_{22}=0$). The potential $\phi(\mathbf{x},t)$ is considered to be a stationary and homogeneous Gaussian stochastic field, with zero average and given two-point Eulerian correlation (EC) function

$$E(\mathbf{x},t) \equiv \langle \phi(\mathbf{x}_1,t_1)\phi(\mathbf{x}_1+\mathbf{x},t_1+t)\rangle \tag{3}$$

where $\langle\cdots\rangle$ denotes the statistical average over the realizations of $\phi(\mathbf{x},t)$. The statistical properties of the space derivatives of the potential are completely determined by those of the potential. They are stationary and homogeneous Gaussian stochastic fields like $\phi(\mathbf{x},t)$. The two-point Eulerian correlations of the derivatives of $\phi(\mathbf{x},t)$ are obtained as derivatives of the potential EC function $E(\mathbf{x},t)$. We introduce the notation $E_{i..;k..}(\mathbf{x},t) \equiv \langle \phi_{i..}(\mathbf{x}_1,t_1)\phi_{k..}(\mathbf{x}_1+\mathbf{x},t_1+t)\rangle$ where $\phi_i(\mathbf{x},t) \equiv (\partial/\partial x_i)\phi(\mathbf{x},t)$ and the subscript of E contains the indices of the derivatives of the potential in $\mathbf{x}_1,t_1$ (left factor) separated by a semicolon from the indices of the derivatives of the potential in $\mathbf{x}_1+\mathbf{x}$, t_1+t (right factor). The absence of indices corresponds to a factor ϕ inside the average. One obtains

$$E_{i..;k..}(\mathbf{x},t) = (-1)^n \frac{\partial}{\partial x_i}\cdots\frac{\partial}{\partial x_k}\cdots E(\mathbf{x},t) \tag{4}$$

where n is the number of derivatives of the first factor $\phi_{i..}(\mathbf{x}_1,t_1)$ inside the above average. In particular, the velocity $\mathbf{v}(\mathbf{x},t)$ is such a stationary and homogeneous Gaussian stochastic field. The correlation of the velocity components and the potential-velocity correlations are obtained using Eqs. (2) and (4). These correlations will be used in the following calculations.

The potential is a continuous function of $\mathbf{x}$ and t in each realization and it determines a unique trajectory as the solution Eq. (1). Starting from the above statistical description of the stochastic potential and from an explicit EC function $E(\mathbf{x},t)$, one has to determine the statistical properties of the trajectories. In particular, the Lagrangian velocity correlation (LVC), defined by

$$L_{ij}(t) \equiv \langle v_i[\mathbf{x}(0),0]v_j[\mathbf{x}(t),t]\rangle \tag{5}$$

for a stationary process, will be evaluated. The mean square displacement $\langle x_i^2(t)\rangle$ and its derivative, the running diffusion coefficient $D_i(t)$, are determined by this function as [22]

$$\langle x_i^2(t)\rangle = 2\int_0^t d\tau L_{ii}(\tau)(t-\tau), \tag{6}$$

$$D_i(t) = \int_0^t d\tau L_{ii}(\tau). \tag{7}$$

This kind of Langevin problem, named in the literature tracer advection or diffusion by continuous movements, is nonlinear due to the space dependence of the potential, which leads to $\mathbf{x}$ dependence of the EC function (3). The importance of the nonlinearity is characterized by the Kubo number defined by

$$K = \frac{V\tau_c}{\lambda_c} = \frac{\tau_c}{\tau_{fl}} \tag{8}$$

where V is the amplitude of the stochastic velocity, τ_c is the correlation time, and λ_c is the correlation length. These parameters appear in the EC function of the velocity as the maximum value at the origin $[V^2=E_{ii}(\mathbf{0},0)]$ and the characteristic decay time and length of this function. The Kubo number is thus the ratio of τ_c to the average time of flight of the particles over the correlation length, $\tau_{fl}=\lambda_c/V$. It measures the particle's capacity of exploring the space structure of the stochastic velocity field before it changes.

For small Kubo numbers the time variation of the velocity field is fast and the particles cannot "see" the space structure of the velocity field. The condition $K \ll 1 (\tau_c \ll \tau_{fl})$ defines the quasilinear regime (or the weak turbulence case) for which the results are well established: the diffusion coefficient is $D_{ql}=(\lambda_c^2/\tau_c)K^2=V^2\tau_c$ and the trajectories have Gaussian distribution.

For $K>1 (\tau_c > \tau_{fl})$ the time variation of the stochastic potential is slow and the trajectories approximately follow the contour lines of $\phi(\mathbf{x},t)$. This produces a trapping effect: the trajectories are confined for long periods in small regions. A typical trajectory shows an alternation of large displacements and trapping events. The latter appear when the particles are close to the maxima or minima of the potential and consist of trajectory winding on almost closed paths. The large displacements are produced when the trajectories are at small absolute values of the potential. Trajectory trapping appears for $K>1$ and becomes stronger as K increases up to the limit of static fields ($K, \tau_c=\infty$) where the trapping is permanent. It determines the decrease of the diffusion coefficient and the change of its dependence on the Kubo number from the Bohm scaling [23,24] $D_B \sim (\lambda_c^2/\tau_c)K = V\lambda_c$ to a trapping scaling $D_{tr} \sim (\lambda_c^2/\tau_c)K^\gamma$ with $\gamma<1$. In the limit of a static potential field (K, $\tau_c \to \infty$) the transport is subdiffusive: $D(t) \sim t^{-\alpha} \to 0$ with $\alpha>0$ and $\langle x^2(t)\rangle \sim t^{1-\alpha}$ grows more slowly than linearly. It can be shown (see Sec. V) that $\gamma=1-\alpha$ and thus the same power law describes the long time behavior of the mean square displacement in a static potential and the dependence on K of the asymptotic diffusion coefficient in a time-dependent potential.

We show here that, in addition to this strong influence on transport, trapping generates trajectory structures similar to fluid vortices. It appears coherently for bundles of neighboring trajectories leading to eddying regions. The statistical characteristics of these trajectory structures are determined.

III. THE NESTED SUBENSEMBLE METHOD

The motion described by Eqs. (1) and (2) has the velocity at any moment perpendicular to the gradient of the potential in the instantaneous position $\mathbf{x}(t)$ and the time variation of the Lagrangian potential is produced only by the explicit time dependence of $\phi(\mathbf{x},t)$ These eqations are of Hamil-

tonian type with the potential as the Hamiltonian function. Thus, for the static case where $\partial\phi/\partial t=0$ ($\tau_c, K\to\infty$), the potential is an invariant of the motion. The trajectories are on the contour lines of the potential and the motion is periodic. For slowly varying or large amplitude potentials such that $\tau_c > \tau_{fl}$ (i.e., $K>1$), $\partial\phi/\partial t$ is small during a time of the order τ_{fl} and there is an approximate invariance of the potential along the trajectory in each realization. Trajectory trapping is essentially related to this invariance of the Lagrangian potential. Thus, a statistical method is adequate for the study of this process if it is compatible with the invariance of the potential.

The main idea in our approach is to study the Langevin equation (1) in subensembles S of realizations of the stochastic field, which are determined by given values of the potential and of the velocity in the starting point of the trajectories:

$$(\mathrm{S}):\ \phi(\mathbf{0},0)=\phi^0,\ \mathbf{v}(\mathbf{0},0)=\mathbf{v}^0. \tag{9}$$

The invariance of the potential appears clearly in S. The probability distribution function of the Lagrangian potential $\phi[\mathbf{x}(t)]$ is

$$P^S(\phi,t)\equiv\langle\delta\{\phi-\phi[\mathbf{x}(t)]\}\rangle_S=\delta(\phi-\phi^0) \tag{10}$$

where $\langle\cdots\rangle_S$ denotes the average taken on the realizations in S. The approximations introduced in the evaluation of the correlation of the Lagrangian velocity must be compatible with Eq. (10). Moreover, the second condition in (9) brings an important simplification in determining the LVC for stationary processes. It actually reduces the two-time correlation of the velocity to the (one-time) average velocity. The stochastic (Eulerian) potential and velocity in a subensemble S defined by condition (9) are Gaussian fields but nonstationary and nonhomogeneous, with space- and time-dependent averages and dispersions. The averages depend on the parameters of the subensemble and are defined by

$$\Phi^E(\mathbf{x},t;S)\equiv\langle\phi(\mathbf{x},t)\rangle_S,\ \mathbf{V}^E(\mathbf{x},t;S)\equiv\langle\mathbf{v}(\mathbf{x},t)\rangle_S \tag{11}$$

where the superscript E is used to underline the Eulerian nature of these quantities. They are equal to the corresponding imposed condition (9) at $\mathbf{x}=\mathbf{0}$ and $t=0$ and decay to zero at large distance and/or time. The mean squares of the potential and velocity fluctuations are zero at $\mathbf{x}=\mathbf{0}$, $t=0$ and increase up to values corresponding to the whole set of realizations at large distance and/or time. The existence of an average Eulerian velocity in the subensemble determines an average motion. The LVC (5) and the time-dependent diffusion coefficient (7) can be expressed as functions of the set of average trajectories in the subensembles S.

This subensemble or conditional analysis of the Langevin equation was introduced in [18] where the decorrelation trajectory method was developed based on an approximation that essentially consists in neglecting the fluctuations of the trajectories in S. The approach presented here is a development of this method, which considers the fluctuations of the trajectories in S and determines their probability distribution function (PDF). We note that similar subensemble averages of the Eulerian stochastic velocity field were studied in [25] with the aim of showing that eddies and structures exist even in isotropic turbulence. Subensemble Lagrangian averages are estimated in [26] on the basis of a rather strong assumption and in [16] for a model of rotating fluid layers.

More precisely, the LVC (5) for the whole set of realizations is obtained by summing up the contributions of each subensemble. The latter can be written as $\langle v_i[\mathbf{x}(0),0]v_j[\mathbf{x}(t),t]\rangle_S=v_i^0V^L(t;\mathrm{S})$ where $\mathbf{V}^L(t;S)\equiv\langle\mathbf{v}[\mathbf{x}(t),t]\rangle_S$ is the average Lagrangian velocity in S and thus

$$L_{ij}(t)=\int\int d\phi^0 d\mathbf{v}^0 P_1(\mathrm{S})v_i^0V_j^L(t;\mathrm{S}). \tag{12}$$

Here $P_1(\mathrm{S})$ is the probability that a realization belongs to the subensemble S and is obtained as

$$P_1(\mathrm{S})=\frac{1}{(2\pi)^{3/2}}\frac{1}{\sqrt{E(\mathbf{0},0)E_{1;1}(\mathbf{0},0)E_{2;2}(\mathbf{0},0)}}\times\exp\left(-\frac{(\phi^0)^2}{2E(\mathbf{0},0)}-\frac{(v_1^0)^2}{2E_{1;1}(\mathbf{0},0)}-\frac{(v_2^0)^2}{2E_{2;2}(\mathbf{0},0)}\right) \tag{13}$$

when $E(\mathbf{x})$ has a maximum at $\mathbf{x}=\mathbf{0}$, as happens in most cases. Equation (12) is an exact equation. Thus the diffusion coefficient (7) is determined by evaluating $\mathbf{V}^L(t;\mathrm{S})$.

Neglecting the fluctuations of the trajectories in S, $\mathbf{V}^L(t;\mathrm{S})$ is approximated in the decorrelation trajectory method [18] with the average Eulerian velocity calculated along the average trajectory:

$$\mathbf{V}^L(t;\mathrm{S})\cong\mathbf{V}^E[\mathbf{X}(t,\mathrm{S}),t;\mathrm{S}] \tag{14}$$

where $\mathbf{X}(t,\mathrm{S})$ is the average trajectory in S, $\mathbf{X}(t,\mathrm{S})\equiv\langle\mathbf{x}(t)\rangle_S$. Then, this average (decorrelation) trajectory in S is determined from the equation

$$\frac{d\mathbf{X}(t,\mathrm{S})}{dt}=\mathbf{V}^E[\mathbf{X}(t,\mathrm{S}),t;\mathrm{S}] \tag{15}$$

so that an explicit expression for $\mathbf{V}^L(t;\mathrm{S})$ is obtained. It was shown that Eq. (15) is of Hamiltonian type with the Hamiltonian function equal to the average Lagrangian potential approximated by $\Phi^E[\mathbf{X}(t,\mathrm{S}),t;\mathrm{S}]$. Thus, in the static case the average trajectories are periodic and evolve on closed paths. The approximation (14) seems to be rather rough but, because it is performed in the subensemble, there are two aspects which contribute to improving its accuracy. One is due to the smaller amplitude of the velocity fluctuations in S, the source of the trajectory fluctuations: it is zero in the starting point of the trajectories and reaches the value corresponding to the whole set of realizations only asymptotically. The second is related to the fact that the trajectories in the subensemble are superdetermined. In addition to the necessary and sufficient initial condition $\mathbf{x}(0)=\mathbf{0}$, they have supplementary initial conditions determined by the definition (9) of the subensembles. This reduces the differences between the trajectories in S and thus their fluctuations. The first description of the trapping process in qualitative agreement with the numerical simulations was obtained using these approximations. However, there are important qualitative aspects that are not obtained from this approximation. The most evident

concerns the average trajectory in the subensemble. In the static case the trajectory in each realization [solution of Eq. (1)] is periodic but the average of such trajectories cannot be periodic [as obtained from Eq. (15)] since they have different periods (distributed around some average value which depends on S). Another aspect is discussed in [20,21] and concerns the average Lagrangian velocity in a biased stochastic potential.

Trajectory fluctuations in the subensembles S are considered here in agreement with the condition (10) by separating the realizations in S into subensembles S2 corresponding to fixed values of the second derivatives of the potential in $\mathbf{x}=\mathbf{0}$, $t=0$:

$$(\mathrm{S2}):\ \phi_{ij}(\mathbf{0},0) \equiv \left.\frac{\partial^2\phi(\mathbf{x},t)}{\partial x_i\,\partial x_j}\right|_{\mathbf{x}=\mathbf{0},t=0} = \phi_{ij}^0 \tag{16}$$

where $ij=11$, 12, 22. The Langevin equation (1) is studied in these subensembles S2. The average trajectory is approximately determined by neglecting trajectory fluctuations in S2. Pushed to the subensembles S2, this approximation is much more accurate than taken in S because the trajectories in S2 are much more superdetermined than those in S: three supplementary initial conditions (16) are added to the initial conditions (9). Moreover, the amplitude of the velocity fluctuations is smaller in S2 than in S. Thus the accuracy of this method is much increased compared to the accuracy of the decorrelation trajectory method. But the main advantage of performing this development consists in the fact that it provides for each subensemble S a collection of trajectories instead of one decorrelation trajectory. It is thus possible to obtain the statistical properties of the trajectories in S by performing averages over the subensembles S2 contained in S. We determine using this nested subensemble procedure the PDF of the trajectories and also the PDF of the distance between two neighboring trajectories. Thus much more statistical information is provided by this method, which permitted us to evidence the existence of coherence in the stochastic trajectories.

We note that this nested subensemble approach can be further developed by introducing subensembles defined by higher order derivatives of the potential, S3, S4, and so on. This systematic expansion satisfies at each order higher than 1 all the conditions required by the invariance of the Lagrangian potential Eq. (10). It is, however, expected that the main statistical properties of the stochastic trajectories in S are already obtained at the second order and that the higher orders contribute with corrections to these results. The nested subensembles S, S2 are considered in this study.

The calculations consist of the following steps. First, the statistical properties of the stochastic potential and velocity, reduced in the subensemble S2 defined by conditions (16) and (9) are derived; namely, the probability that a realization belongs to a subensemble S2 and the subensemble average Eulerian velocity are determined. Then an equation for the average trajectory in S2 is obtained. The statistical properties of the trajectories and of the distance between two trajectories in the upper subensemble S are expressed as functions of the average trajectories in all subensembles S2 contained in S. Finally, the running diffusion coefficient corresponding to the whole statistical ensemble is determined. The calculations are for the static stochastic potential corresponding to the strongest trapping. The transport in a time-dependent potential is discussed in Sec. VI B.

A. Eulerian statistics in the subensemble S2

The (one-point) probability that a realization of the stochastic potential belongs to the subensemble S2 contained in the subensemble S is defined by

$$P_1(\mathrm{S2}) = \frac{\langle \delta[\phi^0-\phi(\mathbf{0})]\delta[\mathbf{v}^0-\mathbf{v}(\mathbf{0})]\prod \delta[\phi_{ij}^0-\phi_{ij}(\mathbf{0})]\rangle}{P_1(\mathrm{S})} \tag{17}$$

where the product Π is for $ij=11$, 12, 22. It is calculated using the Fourier representation of the δ functions and performing the average of the resulting exponential of the stochastic Gaussian quantities (see, e.g., [27]). One obtains after straightforward calculations

$$P_1(\mathrm{S2}) = \frac{1}{(2\pi)^{3/2}}[E_{12;12}(\mathbf{0})c]^{-1/2} \times \exp\left[-\frac{(\phi_{12}^0)^2}{2E_{12;12}(\mathbf{0})} - \frac{a_1^2c_2}{2c} - \frac{a_2^2c_1}{2c} + \frac{a_1a_2c_{12}}{c}\right] \tag{18}$$

where c_i are constants given by

$$c_1 \equiv E_{11;11}(\mathbf{0}) - E_{11;}^2(\mathbf{0})/E(\mathbf{0}),$$

$$c_2 \equiv E_{22;22}(\mathbf{0}) - E_{22;}^2(\mathbf{0})/E(\mathbf{0}),$$

$$c_{12} \equiv E_{11;22}(\mathbf{0}) - E_{11;}(\mathbf{0})E_{22;}(\mathbf{0})/E(\mathbf{0}),$$

$$c = c_1c_2 - c_{12}^2, \tag{19}$$

and a_i are essentially the parameters ϕ_{ii}^0 of the subensemble S2,

$$a_1 \equiv \phi_{11}^0 - \phi^0 E_{11;}(\mathbf{0})/E(\mathbf{0}),$$

$$a_2 \equiv \phi_{22}^0 - \phi^0 E_{22;}(\mathbf{0})/E(\mathbf{0}). \tag{20}$$

The average Eulerian potential in the subensemble S2, $\Phi^E(\mathbf{x};\mathrm{S2}) \equiv \langle\phi(\mathbf{x})\rangle_{S2}$, is determined by the conditional average corresponding to Eq. (16):

$$\Phi^E(\mathbf{x};S2) = \frac{\langle \phi(\mathbf{x})\delta[\phi^0-\phi(\mathbf{0})]\delta[\mathbf{v}^0-\mathbf{v}(\mathbf{0})]\prod \delta[\phi_{ij}^0-\phi_{ij}(\mathbf{0})]\rangle}{P_1(\mathrm{S})P_1(\mathrm{S2})}. \tag{21}$$

This average is calculated by introducing the Fourier representation of the δ functions which leads to the average of $\phi(\mathbf{x})$ multiplied with an exponential of a linear combination of $\phi(\mathbf{0})$, $\mathbf{v}(\mathbf{0})$ and $\phi_{ij}(\mathbf{0})$. It can be written as the derivative at a parameter β taken at $\beta=0$ of the average of the exponential of the above linear combination with an additional term $\beta\phi(\mathbf{x})$. One obtains after performing the inverse Fourier transforms

$$\Phi^E(\mathbf{x};\mathrm{S2}) = -\frac{\left[E(\mathbf{x})\,\partial/\partial\,\phi^0 + E_{i;}(\mathbf{x})\,\partial/\partial\,\phi_i^0 + E_{ij;}(\mathbf{x})\,\partial/\partial\,\phi_{ij}^0\right]P_1(\mathrm{S})P_1(\mathrm{S2})}{P_1(\mathrm{S})P_1(\mathrm{S2})}, \tag{22}$$

which can be written explicitly as

$$\begin{aligned}\Phi^E(\mathbf{x};S2) = \frac{E(\mathbf{x})}{E(\mathbf{0})}\Bigg[\phi^0 + \frac{a_1[E_{22;}(\mathbf{0})c_{12} - E_{11;}(\mathbf{0})c_2]}{c} \\ + \frac{a_2[E_{11;}(\mathbf{0})c_{12} - E_{22;}(\mathbf{0})c_1]}{c}\Bigg] + \frac{E_{2;}(\mathbf{x})}{E_{2;2}(\mathbf{0})}v_1^0 \\ - \frac{E_{1;}(\mathbf{x})}{E_{1;1}(\mathbf{0})}v_2^0 + \frac{E_{12;}(\mathbf{x})}{E_{12;12}(\mathbf{0})}\phi_{12}^0 \\ + \frac{E_{11;}(\mathbf{x})(a_1c_2 - a_2c_{12})}{c} + \frac{E_{22;}(\mathbf{x})(a_2c_1 - a_1c_{12})}{c}.\end{aligned} \tag{23}$$

The subensemble S2 average potential (23) equals ϕ^0 at $\mathbf{x}=\mathbf{0}$, $t=0$ and it decays to zero at large $\mathbf{x}$, like the average Eulerian potential in the upper subensemble S. Its expression is more complicated and depends on the second order derivatives ϕ_{ij}^0 that label S2. The potential considered only in the realizations in the subensemble S2 is a nonstationary and nonhomogeneous Gaussian field having a space-time-dependent average.

As in the whole ensemble and as in S, the statistical properties of the velocity field in the subensemble S2 are deduced from those of the potential in S2. The velocity in the subensemble S2 is a nonstationary and nonhomogeneous Gaussian stochastic field having a space-time-dependent average. This average Eulerian velocity is calculated by the same procedure used for the potential (23). The relation (2) between velocity and potential in each realization holds between the respective average quantities calculated in the nested subensembles. It was obtained in the subensemble S in [18], and it can be shown that

$$V_i^E(\mathbf{x};\mathrm{S2}) = \epsilon_{ij}\frac{\partial\,\Phi^E(\mathbf{x};\mathrm{S2})}{\partial\,x_j}. \tag{24}$$

Thus the average velocity in the subensemble S2 is divergence-free: $\boldsymbol{\nabla}\cdot\mathbf{V}^E(\mathbf{x};\mathrm{S2})=0$.

It is interesting to note that the potential and the velocity in the subensembles S and S2 are deterministic quantities in $\mathbf{x}=\mathbf{0}$ [$\phi(\mathbf{0})=\phi^0$, $\mathbf{v}(\mathbf{0})=\mathbf{v}^0$ for all realizations in S, and thus also in S2]. As $|\mathbf{x}|$ grows, the average values decay to zero and the fluctuations build up progressively and eventually become the same as in the global statistical ensemble. The amplitude of the fluctuations at a point $\mathbf{x}$ is smaller in the subensemble S2 than in the subensemble S.

This nested subensemble procedure evidences, in the zero-average stochastic velocity field, a *set of average velocities* (corresponding to each subensemble). They depend on the statistical characteristics of the velocity field (the correlation and the constraint imposed in the problem, i.e., the zero-divergence condition). The following relation holds between the S2 average velocities and the S average velocity:

$$\mathbf{V}^E(\mathbf{x};\mathrm{S}) = \int d\phi_{11}^0 d\phi_{12}^0 d\phi_{22}^0 P_1(\mathrm{S2})\mathbf{V}^E(\mathbf{x};\mathrm{S2}). \tag{25}$$

Similar equations can be written for all statistical quantities defined in the nested subensembles.

B. Average trajectory in the subensemble S2

The average Eulerian velocity (24) determines an average displacement in the subensemble S2, $\mathbf{X}(t;\mathrm{S2})$. It is the time integral of the average Lagrangian velocity in S2, $\mathbf{V}^L(t;\mathrm{S2})$. The latter is evaluated by neglecting the fluctuations of the trajectories in the subensemble S2 as

$$\mathbf{V}^L(t;\mathrm{S2}) \cong \mathbf{V}^E[\mathbf{X}(t;\mathrm{S2});\mathrm{S2}]. \tag{26}$$

With this approximation the average Lagrangian potential in S2 is $\langle\varphi[\mathbf{x}(t)]\rangle_{S2} \cong \Phi^E[\mathbf{X}(t;\mathrm{S2});\mathrm{S2}]$. Due to Eq. (24) a Hamiltonian equation is obtained for $\mathbf{X}(t;\mathrm{S2})$:

$$\frac{dX_i(t;\mathrm{S2})}{dt} = \varepsilon_{ij}\frac{\partial}{\partial X_j}\Phi^E[\mathbf{X}(t;\mathrm{S2});\mathrm{S2}]. \tag{27}$$

The potential calculated along the solution of Eq. (27) with the initial condition $\mathbf{X}(0;\mathrm{S2})=\mathbf{0}$ is invariant and independent of the parameters of S2:

$$\Phi^E[\mathbf{X}(t;\mathrm{S2});\mathrm{S2}] = \phi^0 \tag{28}$$

at any time and for all subensembles S2 included in S.

C. Lagrangian statistics in the subensemble S

The nested subensemble method provides for a subensemble S an ensemble of trajectories, the average trajectories $\mathbf{X}(t;\mathrm{S2})$, one for each subensemble S2 contained in S. A weighting factor $P_1(S2)$ is attributed to each trajectory

$\mathbf{X}(t;\mathrm{S2})$. The Lagrangian statistics in the subensemble S is obtained by performing weighted averages over these trajectories. So the average Lagrangian velocity in S, $\mathbf{V}^L(t;\mathrm{S})$, is determined by averaging $\mathbf{V}^L(t;\mathrm{S2})$ obtained from Eqs. (26) and (27) over all subensembles S2 contained in S,

$$\mathbf{V}^L(t;S) = \int d\phi_{11}^0 d\phi_{12}^0 d\phi_{22}^0 P_1(\mathrm{S2}) \mathbf{V}^E[\mathbf{X}(t;\mathrm{S2});\mathrm{S2}]. \tag{29}$$

The average trajectory in the subensemble S, $\mathbf{X}(t;\mathrm{S}) \equiv \langle \mathbf{x}(t) \rangle_S$, is determined by averaging $\mathbf{X}(t;\mathrm{S2})$, the solution of Eq. (27):

$$\mathbf{X}(t;\mathrm{S}) = \int d\phi_{11}^0 d\phi_{12}^0 d\phi_{22}^0 P_1(\mathrm{S2}) \mathbf{X}(t;\mathrm{S2}). \tag{30}$$

The dispersion of the trajectories in S, $d_i(t;\mathrm{S}) \equiv \langle (x_i(t) - \mathbf{X}(t;\mathrm{S}))^2 \rangle_S$, is

$$d_i(t;S) = \int d\phi_{11}^0 d\phi_{12}^0 d\phi_{22}^0 P_1(\mathrm{S2}) X_i^2(t;\mathrm{S2}) - X_i^2(t;\mathrm{S}). \tag{31}$$

The PDF for the trajectories in S is determined by integrating the PDF in the subensemble S2, which in this approximation is $\delta[\mathbf{x} - \mathbf{X}(t;S2)]$,

$$P^S(\mathbf{x},t) = \int d\phi_{11}^0 d\phi_{12}^0 d\phi_{22}^0 P_1(\mathrm{S2}) \delta[\mathbf{x} - \mathbf{X}(t;\mathrm{S2})]. \tag{32}$$

We note that Eqs. (30)–(32) are exact.

The PDF for the Lagrangian potential $\phi[\mathbf{x}(t)]$ in the subensemble S obtained by this method equals $\delta(\phi - \phi^0)$ since the potential is equal to ϕ^0 on all trajectories considered in the average. This shows that the approximation (26) introduced in this method ensures entirely the statistical properties of the Lagrangian potential.

The statistical properties of the distance between two trajectories in a subensemble S, $\delta(t) \equiv \mathbf{x}'(t) - \mathbf{x}(t)$ with $\mathbf{x}'(0) = \delta_0$ and $\mathbf{x}(0) = \mathbf{0}$, can also be determined using the average over the subensembles S2. The average trajectory in S2, $\mathbf{X}'(0;\mathrm{S2}) \equiv \langle \mathbf{x}'(t) \rangle_{S2}$, is the solution of Eq. (27) with the initial condition $\mathbf{X}'(0;\mathrm{S2}) = \delta_0$. The average, the dispersion, and the PDF of $\delta(t)$ in a subensemble S are determined by equations similar to Eq. (30)–(32) where $\mathbf{X}(t;\mathrm{S2})$ is replaced by $\mathbf{X}'(t;\mathrm{S2}) - \mathbf{X}(t;\mathrm{S2})$.

D. Running diffusion coefficient

The correlation of the Lagrangian velocity in the whole set of realizations is determined using Eqs. (12) and (29). The running diffusion coefficient (7) is obtained by integrating the LVC (12) as

$$D_i(t) = \int \int d\phi^0 d\mathbf{v}^0 P_1(S) v_i^0 X_i(t;S). \tag{33}$$

In the case of an isotropic stochastic field, the integral over the orientation of the velocity $\mathbf{v}^0$ can be performed analytically [18] and one obtains for the static case

$$D(t) = \frac{1}{\sqrt{2\pi}} \frac{1}{\sqrt{E(\mathbf{0},0) E_{1;1}(\mathbf{0},0)}} \int_0^\infty d\phi^0 \int_0^\infty du\, u^2 \times \exp\left(- \frac{(\phi^0)^2}{2E(\mathbf{0},0)} - \frac{u^2}{2E_{1;1}(\mathbf{0},0)} \right) X_1(t;\mathrm{S}) \tag{34}$$

and

$$L(t) = D'(t), \tag{35}$$

where $X_1(t;\mathrm{S})$ is the component of the average trajectory along $\mathbf{v}^0$, determined from Eq. (30), and $D'(t)$ is the derivative of the function $D(t)$. We note that the same analytical expression for $D(t)$ in terms of the average trajectory $X_1(t;\mathrm{S})$ is obtained in [18] by means of the decorrelation trajectory method. The difference is that the average trajectory was determined there as a solution of a Hamiltonian equation while here it is the average (30) of the average trajectories in S2.

IV. DISCUSSION AND EXPLICIT CALCULATIONS

The nested subensemble method actually is based on the classification of stochastic trajectories in groups (subensembles) according to some resemblance between them. The most important criterion in this classification is the value of the potential at the starting point of the trajectories. All trajectories contained in such a group evolve on contour lines with the same value of the potential. Consequently, their paths and periods are statistically similar in the sense that they have an average size and period. Thus this condition determines a global resemblance of the trajectories (extended at long time). This condition is imposed beginning with the first level of classification (in the subensembles S). Other criteria of the classification are the velocity and the derivatives of the velocity in the origin. These are not conserved quantities and thus they influence the shape of the trajectory only at small time for time intervals that grow with the number of imposed conditions. The value of the initial velocity is fixed in the subensemble S; then each subensemble S is divided in smaller subensembles S2 according to the value of the derivatives of the velocity (second derivatives of the potential). This classification can continue in principle and at each step the resemblance of the trajectories contained in a group is increased and the number of groups grows. The approximation consists in neglecting the differences between the trajectories in a group. With this condition it is possible to determine an average trajectory for each subensemble. Thus the nested subensemble method determines a set of trajectories [$\mathbf{X}(t;\mathrm{S2})$ for the second order considered here] and a weighting factor for each one. Then, the statistical properties of the stochastic trajectory are obtained by performing weighted averages over these trajectories. Except for some special case, the trajectories $\mathbf{X}(t;\mathrm{S2})$ have to be numerically calculated by solving the Hamiltonian system (27). This procedure appears to be very similar to a direct numerical study of the simulated trajectories. There are, however, essential differences. The average trajectories are obtained from a rather smooth and simple time-independent Hamiltonian. They are periodic functions and thus are calculated

only for a period. The number of trajectories is much smaller than in the numerical study due to the weighting factor determined analytically. This very much reduces the calculation time, such that it can be performed on a PC. Moreover, such a calculation performed for a static stochastic potential with a given EC determines the solution for the time-dependent potential with arbitrary time factor in the EC (see Sec. VI B).

The nested subensemble method determines the statistics of the trajectories in subensembles S and the LVC for tracers advected in a Gaussian stochastic potential with given EC. The main condition for using this method is that the transport is stationary, which usually corresponds to stationary and homogeneous stochastic potentials. The time-dependent diffusion coefficient (34) is obtained for an isotropic potential but this is not a restriction for this method. The above calculations are for a static potential but they can be extended to the time-dependent case (see Sec. VI B).

We have developed an algorithm for calculating the statistical characteristics of the trajectories in subensembles S and the running diffusion coefficient (34) for given EC of the potential. The solutions of Eqs. (27) are calculated for a period using a variable integration step monitored by the precision obtained for the potential. Precisions of the order of 10^{-3}–10^{-4} ensures the stability of the calculated $D(t)$. The order of performing the integrals in Eq. (34) appears to be important. The integral over u is first calculated. This parameter is factorized in the expression of the average Eulerian potential in S2 [Eq. (23)] and is introduced in the time variable $\tau=ut$ Thus, only the trajectories with $u=1$ need to be calculated. The values of the function $X_1(ut;\mathrm{S2})$ are determined from the trajectory obtained from Eq. (27) with $u=1$ by interpolation and using the periodicity. The integration step du is determined at each time such that a large enough number of points (30–50) exists on each period. When there are more than about 50 periods on the range of u the integration is not performed because its value is negligible. The next integrations are over ϕ^0_{12}, ϕ^0_{11}, and ϕ^0_{22}. They are calculated on constant step meshes with 31–61 points. Last is performed the integral over ϕ^0. Due to trajectory trapping, the range of this integral is continuously reduced as time increases ($\phi^0_{\max}\to 0$ when $t\to\infty$). The range of this integral is determined as a function of time. The calculations start with a large value of $\phi^0_{\max}$, as obtained from the exponential factor. At the time when the integrand becomes approximately zero on half of this range $\phi^0_{\max}$ is reduced and the integration of the trajectories is taken again from $t=0$ for the new values of ϕ^0. The mesh for ϕ^0 has variable steps that increase toward large values of ϕ^0 because the function has strong variations at small ϕ^0. The tests performed with this code have shown that the numerical calculations are rather fast and accurate and they can be advanced up to large values of time. For instance, using the decorrelation trajectory method the duration of the calculation of $D(t)$ up to time of the order 10^2 is of the order of a few seconds on the usual PC. Using the nested subensemble method the calculation time is of the order of 10 h because the number of calculated trajectories increases by a factor of 10^4.

V. TRAJECTORY STRUCTURES

We present in this section typical results obtained for one- and two-particle statistics in a subensemble S. We need to specify the EC function of the stochastic potential (3), which we choose as

$$E(\mathbf{x}) = \frac{1}{1+(x_1^2+x_2^2)/2}. \tag{36}$$

This is the EC function of a normalized stochastic potential with amplitude $E(\mathbf{0})=1$, $\lambda_c=1$, and $\tau_{fl}=1$. Thus in Figs. 1–7 the time unit is τ_{fl} and the length unit is λ_c. The velocity $\mathbf{v}^0$ that defines the subensembles S is taken along the x_1 axis.

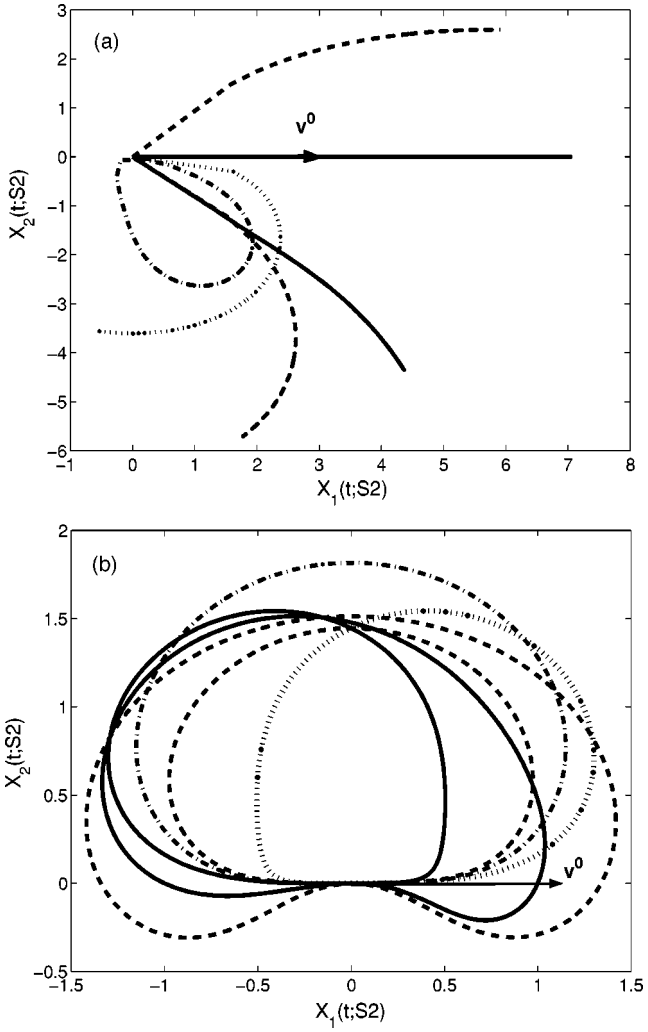

FIG. 1. Examples of paths of the average trajectories in subensembles S2 obtained from Eq. (27) for several values of ϕ^0_{ij} and for $\phi^0=0$, $u=2$ (a) and $\phi^0=1$, $u=2$ (b).

The average trajectory in the subensembles S2, the solution of Eq. (27), is a periodic function of time and evolves on a closed path for most of the subensembles S2. As seen in Fig. 1, there is a clear difference between the trajectories corresponding to small $|\phi^0|$ [Fig. 1(a) for $\phi^0=0$] and large $|\phi^0|$ [Fig. 1(b) for $\phi^0=1$]. In the first case there are open trajectories, large displacements, and large periods for the closed paths. In the second case the trajectories have small size and their periods are much smaller. This is due to the fact that at small $|\phi^0|$ the trajectories are close to the separatrix of the Hamiltonian (23) while at large $|\phi^0|$ they are close

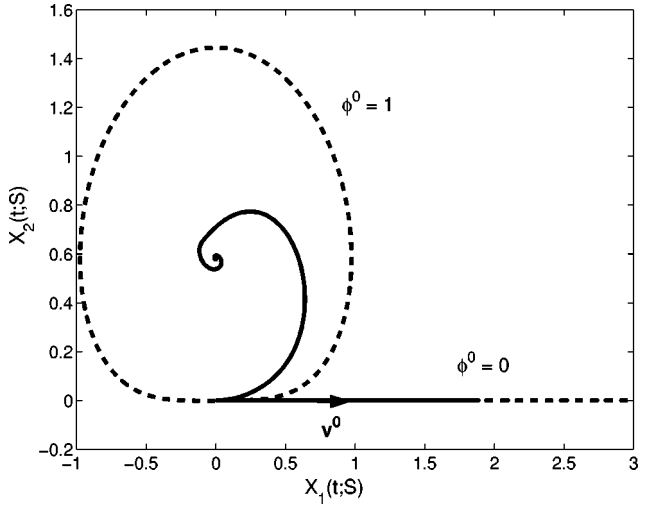

FIG. 2. Examples of paths of the average trajectories in subensembles S obtained from Eq. (30) (continuous lines). The results obtained with the decorrelation trajectory method are also plotted for comparison (dashed lines).

to its elliptic points. The size of the path and the period of the trajectory depend on the six parameters that define the nested subensembles S, and S2.

The average trajectory in the upper subensemble S is obtained from Eq. (30). Typical average trajectories in S are presented in Figs. 2 and 3. These trajectories are not periodic. They evolve on spiral shaped paths, except for the subensemble with $\phi^0=0$ which yields a continuous displacement along $\mathbf{v}^0$ (Fig. 2). The size of the paths depends on the parameters of S, ϕ^0 and $u\equiv|\mathbf{v}^0|$: it is large for small $|\phi^0|$ and large u and it decreases as $|\phi^0|$ increases. The displacement along the initial velocity $\mathbf{v}^0$ decays to zero in a characteristic time τ_s while the displacement perpendicular to $\mathbf{v}^0$ saturates at a finite value whose sign is the same as the sign of ϕ^0 [Fig. 3(b)]. The saturation time τ_s depends on the parameters of the subensemble S. It increases when $|\phi^0|$ decreases (as the size of the paths) and when $\phi^0\to 0$ it becomes infinite. Thus the average trajectories in S obtained here are completely different from those obtained by means of the decorrelation trajectory method [18]. The latter are periodic functions of time and their paths are closed (see Fig. 2 for comparison). This means that the fluctuations of the trajectories have a strong influence on the average trajectory in S. They determine the time saturation of the average trajectory in S by the mixing of the closed periodic trajectories.

The dispersion of the trajectories in the subensemble S obtained from Eq. (31) is presented in Fig. 3 as a function of time for $\phi^0=0$ [Fig. 3(a)] and $\phi^0=1$ [Fig. 3(b)]. One can see that in the first case the dispersion continuously increases [Fig. 3(a)] while in the second case it saturates after a more complicated evolution [Fig. 3(b)]. The saturation time is the same as for the average trajectory. The amplitude of the trajectory fluctuations is comparable with the average displacement. The small time evolution of the dispersion is very slow, approximately as t^4, and thus much slower than the usual ballistic regime $d_i\sim t^2$. This is due to the fluctuations of the Eulerian velocity in S which are small near $\mathbf{x}=\mathbf{0}$.

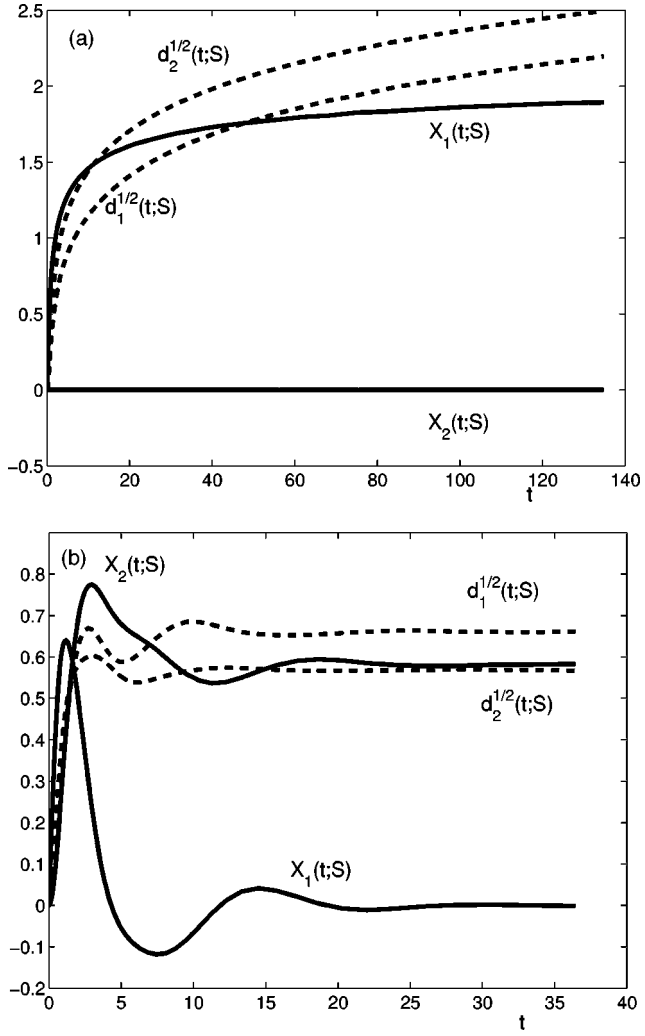

FIG. 3. Time evolution of the average trajectory and of the dispersion [Eq. (31)] in two subensembles S: one with $\phi^0=0$, $u=1$ (a) and the other with $\phi^0=1$, $u=1$ (b).

The trajectories in the subensemble S are Gaussian at small time $t\ll\tau_{fl}$ but their distribution is strongly modified as time increases. The PDF obtained from Eq. (32) is represented in Fig. 4. Important differences can be observed between the subensembles with $\phi^0\cong 0$ [Fig. 4(a)] and those with large $|\phi^0|$ [Fig. 4(b)]. In the first case the PDF is symmetric around $\mathbf{v}^0$; it develops a narrow maximum at $\mathbf{x}=\mathbf{0}$ and an annulus that expands continuously in the direction of $\mathbf{v}^0$ as time increases [Fig. 4(a)]. The velocity of this part of the trajectories is larger than the average velocity. The path of the average displacement is also represented in Fig. 4(a) (red line). The end point of this curve is the average position at the moment corresponding to the representation of the PDF ($t=100\tau_{fl}$). It is located between the two maxima of the PDF in a region where the latter is practically zero. The PDF for subensembles with large $|\phi^0|$ is completely different. It saturates in a time τ_s at a function that has a narrow maximum in $\mathbf{x}=\mathbf{0}$ and extends only on a small region (with $x_2>0$ for $\phi^0>0$) [see Fig. 4(b)].

Typical results obtained for the second moment of the relative displacement $\delta(t)\equiv\mathbf{x}'(t)-\mathbf{x}(t)$, $\Delta_i(t)\equiv\langle\delta_i^2(t)\rangle_S$, are

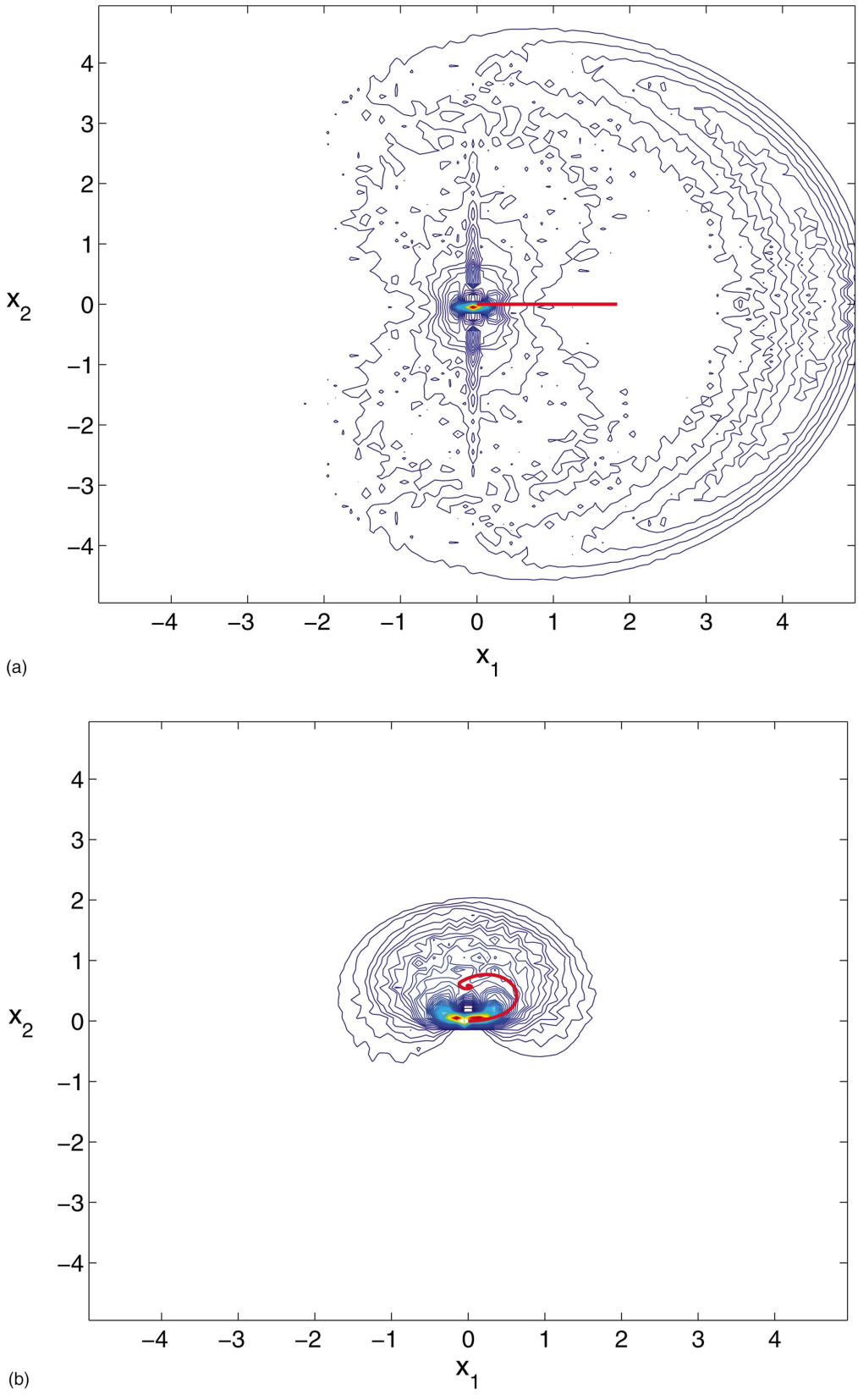

FIG. 4. (Color) Contour plot of the PDF [Eq. (32)] of the trajectories at time t in two subensembles S: one with $\phi^0=0$, $u=1$ for $t=100\tau_{fl}$ (a) and the other with $\phi^0=1$, $u=1$ for $t=30\tau_{fl}$ (at saturation) (b). The path of the average trajectory is also represented (red line) on the interval $[0,t]$.

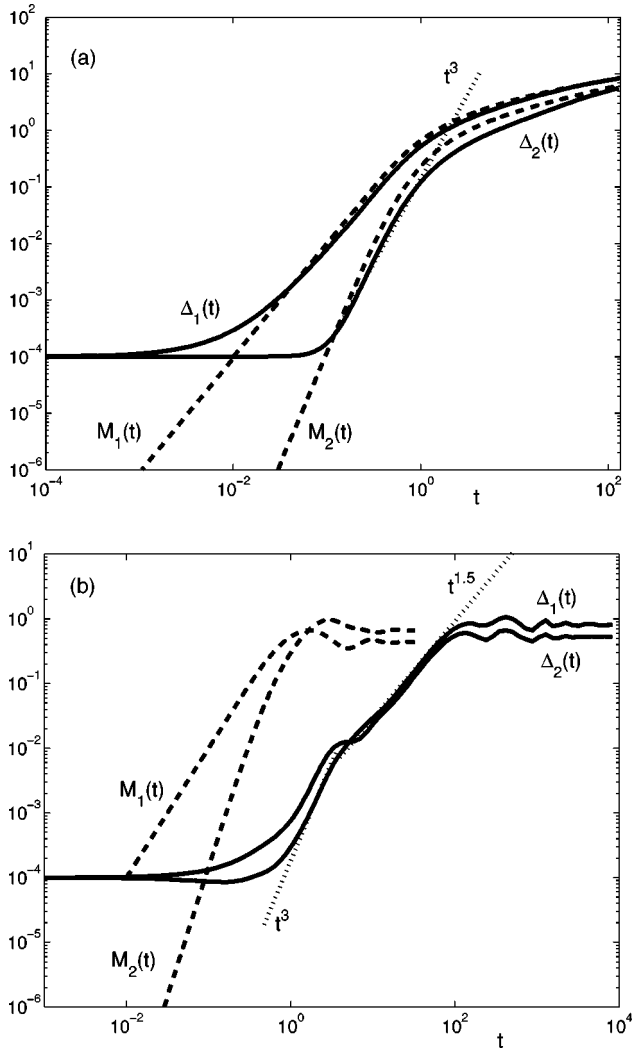

FIG. 5. The second moments of the relative displacement $\Delta_i(t)$ (continuous lines) compared to $M_i(t) \equiv \langle x_i^2(t) \rangle_S$ (dashed lines) in two subensembles S: one with $\phi^0 = 0$, $u = 1$ (a) and the other with $\phi^0 = 1$, $u = 1$ (b).

presented in Fig. 5 (continuous lines) compared with the second moments of the trajectories $M_i(t) \equiv \langle x_i^2(t) \rangle_S$ (dashed lines). In the subensembles with large $|\phi^0|$ [Fig. 5(b)], the evolution of $\Delta_i(t)$ shows that it maintains for a long time the initial value δ_0^2 and that it reaches values comparable with $M_i(t)$ only after a very long time (of the order of $100\tau_{fl}$). The relative motion is governed by the Richardson law $\Delta_i(t) \sim t^3$ only for $t < \tau_s$. After the saturation of M_i at τ_s, the distance between trajectories increases slowly, approximately as $\Delta_i(t) \sim t^{1.5}$, up to the moment when it saturates at a value comparable with that of M_i. Thus the relative motion is strongly hindered by trapping, which shows a very strong degree of coherence of the stochastic trajectories. The clump effect is thus very strong for the trapped trajectories. On the contrary, the clump effect is very weak (practically absent) for the trajectories which are in the subensembles with $\phi^0 \cong 0$. As seen in Fig. 5(a), $\Delta_i(t)$ have values comparable to those of $M_i(t)$ from the first stage of the evolution, at time much smaller τ_{fl}. Thus, the trapping has a strong influence on the statistical characteristics of the relative motion. It produces an anomalous clump effect. In the absence of trapping the small time evolution of $\Delta_i(t)$ is exponential for a very small initial separation δ_0 and is given by the Richardson law for larger δ_0 [5,6]. The process of trajectory trapping strongly enhances the clump effect, determining a much weaker increase of $\Delta_i(t)$ and a very long clump lifetime, much larger than τ_{fl} and than the saturation time τ_s [Fig. 5(b)].

The PDF of $\delta(t)$ in a subensemble S shows that the relative motion is not Gaussian. In the case of large $|\phi^0|$, the PDF remains very localized around zero and saturates [Fig. 6(b)]. In the case of free trajectories ($\phi^0 \cong 0$), the PDF has a more complicated shape and extends continuously. At large times it is similar to the PDF of the trajectories [Fig. 6(a)].

Thus the statistical characteristics of the trapped trajectories (corresponding to subensembles S with a large values of $|\phi^0|$) are completely different from those of free rajectories (obtained in subensembles with $\phi^0 \cong 0$). The average, the dispersion, and the PDF of trapped trajectories and of the distance between them saturate. This shows that there is a quasicoherent motion in such subensembles consisting in trajectory rotation on closed paths, with localized PDFs and small saturated dispersion. The trajectories form structures similar to fluid vortices. These structures or eddying regions are permanent in static stochastic potentials. The saturation time τ_s represents the average time necessary for the formation of the structure. The average size of the structure is represented by the asymptotic average displacement $|\mathbf{X}(t;\mathrm{S})|$ at $t \gg \tau_s$. The dispersion of the trajectories in the structure is given by the asymptotic value of $d_i(t;\mathrm{S})$. We have found that these characteristic parameters of the trajectory structures depend on the parameters of the subensemble S. The size, the dispersion, and the buildup time of the structures increase when $|\phi^0|$ decreases and go to infinity at $\phi^0 = 0$. The time evolution of the relative square displacement $\mathbf{\Delta}(t)$ is very slow, showing that neighboring particles have a coherent motion for a long time, much longer than τ_s.

For free trajectories (that move along contour lines of the potential with $\phi^0 \cong 0$), the average and the dispersion continuously increase and the PDF continuously spreads. The clump effect is absent and the relative motion becomes rapidly incoherent, after a time interval smaller than τ_{fl}. Only these trajectories that are not contained in the structures contribute to the transport.

VI. TRANSPORT

A. Static stochastic potential

The Lagrangian velocity correlation and the time-dependent diffusion coefficient for the whole ensemble of trajectories are determined from Eqs. (35) and (34). The integral over the parameters of the subensembles S of the average displacement in S has to be calculated. Since $X_1(t;\mathrm{S})$ decays to zero in a time $\tau_s(\mathrm{S})$, the trajectory structures have only a transient contribution to the running diffusion coefficient. At times larger than $\tau_s(\mathrm{S})$ the contribution of the subensemble S vanishes. As time increases the diffusion coefficient $D(t)$ is determined by a smaller and smaller number of

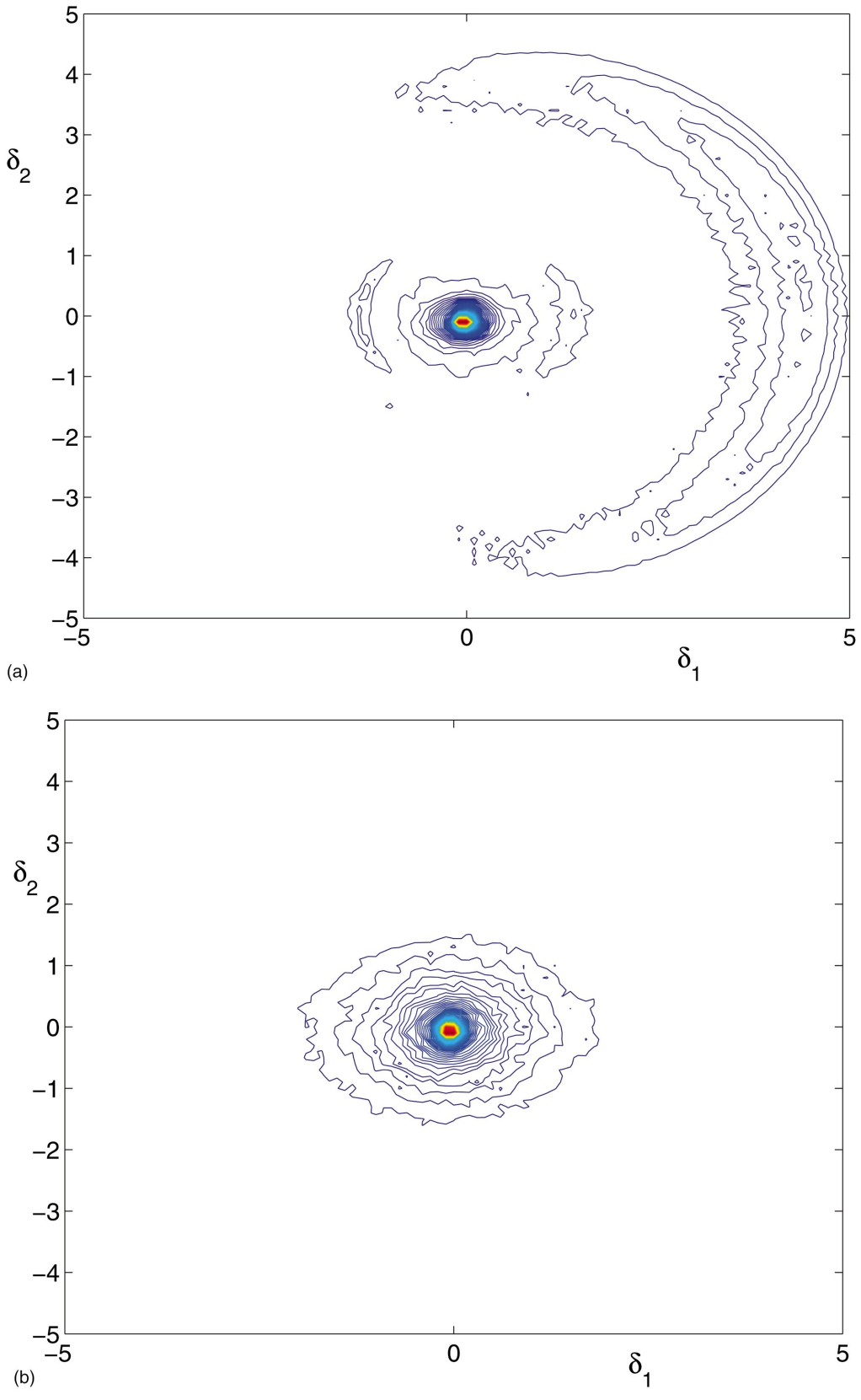

FIG. 6. (Color) Contour plot of the PDF of the distance $\delta(t)$ in two subensembles S: one with $\phi^0=0$, $u=1$, $t=100\tau_{fl}$ (a) and the other with $\phi^0=1$, $u=1$, $t=7000\tau_{fl}$ (at saturation) (b).

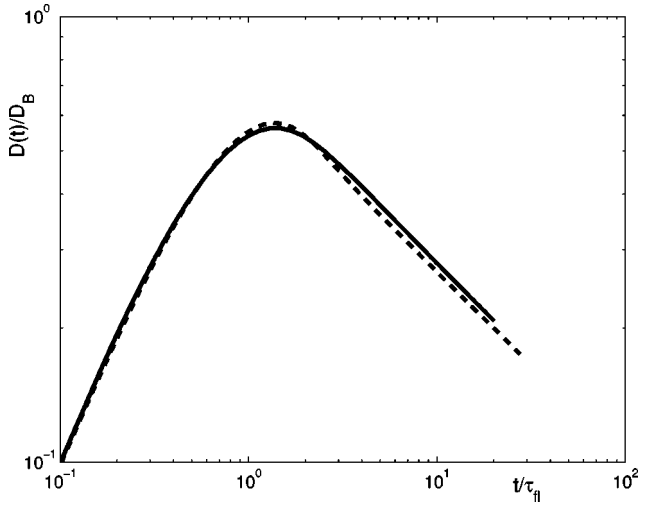

FIG. 7. The time-dependent diffusion coefficient $D(t)$ obtained from Eq. (34) with the nested subensemble method (continuous line) compared with the result of the decorrelation trajectory method (dashed line).

trajectories, those contained in large structures with large saturation time. The results obtained for $D(t)$ are presented in Fig. 7 where the dimensionless function $F(t) \equiv D(t)/D_B$ is plotted (continuous line). The transport is subdiffusive in such a static stochastic potential. One can observe the change that appears at $t \gtrsim \tau_{fl}$. The running diffusion coefficient begins to decrease and eventually goes to zero. A power law decay was obtained at $t > \tau_{fl}$ as $D(t) \sim (t/\tau_{fl})^{-0.42}$. The LVC becomes negative at $t \simeq \tau_{fl}$ and after a minimum it has a long negative algebraic tail that decays to zero. This shows memory persistence in the stochastic process. The positive and the negative parts of $L(t)$ have equal time integrals such that $\int_0^t L(\tau)d\tau = D(t) \to 0$. The shape of the LVC was analyzed in [19], where it was shown that this stochastic process is unstable in the sense that any weak perturbation determines a strong modification of the transport and anomalous diffusion regimes with diffusion coefficients which increase with the increase of the perturbation strength. The mean square displacement is $\langle x^2(t) \rangle \sim t^{0.58}$ and thus the process is subdiffusive.

The result obtained for $D(t)$ with the decorrelation trajectory method is also plotted in Fig. 7 (dashed line). It is surprisingly close to the result of the nested subensemble method although the two methods yield completely different average trajectories in the subensembles S (Fig. 2). This shows that by introducing the subensembles S2 in the nested subensemble method a strong qualitative improvement of the statistical results in the next upper subensemble S is obtained and only a small correction at the level of the whole set of realizations. It is thus expected that the development of the method by introducing higher order derivatives and the corresponding nested subensembles S3, S4, etc., would yield only small corrections for the physically interesting results that concern the diffusion coefficient $D(t)$ and the statistical properties of the trajectory structures. This nested subensemble method appears to be quickly convergent. This is a consequence of the fact that the mixing of periodic trajectories, which characterizes this nonlinear stochastic process, is directly described at each order of our approach. The results obtained in first order (the decorrelation trajectory method) for $D(t)$ are thus validated by the present second order calculations.

B. Time-dependent stochastic potential

For a time-dependent potential $\phi(\mathbf{x},t)$ (finite τ_c and K), it is also possible to apply the nested subensemble method following the same procedure as above. A very simple analytical solution is obtained when the stochastic potential has independent time and space variations such that its EC function is $E(\mathbf{x})h(t)$. In this case, the average Eulerian potential in the subensemble S is given by Eq. (23) multiplied with the factor $h(t)$. This factor is transmitted to the average Eulerian velocity in S (24) and it appears in Eq. (27) for the average trajectory in S2. A change of variable from t to

$$\theta(t) = \int_0^t h(\tau)d\tau \tag{37}$$

can be performed in Eq. (27) and thus the average trajectory in S2 for a time-dependent potential can be written in terms of the average trajectory for the static case as $\mathbf{X}(\theta(t);\ \mathrm{S2})$. The argument $\theta(t)$ determined by the time dependence of the potential is $\theta(t) \cong t$ at small t and saturates at a constant which is the decorrelation time, $\theta(t) \to \tau_c$. The same expression (34) is eventually obtained for the time-dependent diffusion coefficient but with $X_1(t;\ \mathrm{S})$ replaced by $X_1(\theta(t);\ \mathrm{S})$. Thus the diffusion coefficient in the time-dependent case is

$$D^{td}(t) = D[\theta(t)], \tag{38}$$

where D is the diffusion coefficient for the static potential with the same space correlation, given by Eq. (34). The limit for $t \to \infty$ is finite which shows that the transport is diffusive in a time-dependent stochastic potential and the asymptotic diffusion coefficient is

$$D^{td} = D(\tau_c) = D_B F(\tau_c). \tag{39}$$

This equation shows that the asymptotic diffusion coefficient is determined by the time-dependent diffusion coefficient $D(t)$ corresponding to the static potential [$F(t)$ is the function plotted in Fig. 7 and represents the normalized diffusion coefficient in the static potential and $D_B = (\lambda_c^2/\tau_c)K = V\lambda_c$ is the Bohm diffusion coefficient obtained when trajectory trapping is neglected].

We note that Eqs. (38) and (39) are valid for all values of the Kubo number K. In the limit of small K, the quasilinear result is recovered from Eq. (39) and, at large K, D^{td} is reduced compared to the Bohm diffusion coefficient by a factor $F(K) < 1$ which accounts for trajectory trapping. For the above EC function of the potential, Eq. (39) gives the large K scaling law $D^{td} \approx (\lambda_c^2/\tau_c)K^{\gamma}$ with $\gamma = 0.58$. The exponent γ depends on the EC function of the potential, namely, on its space dependence at large distances. It is not a fixed value as in the estimation based on percolation theory [17]. A study of the effect of the EC function of the potential on the scaling of the diffusion coefficient is presented in [28].

Thus, the results obtained for the static case permit us to determine the asymptotic diffusion coefficient in a time-dependent stochastic potential. This property appears in the results of the nested subensemble method (and in the decorrelation trajectory method) but it is possible to demonstrate in general that the time dependence of the diffusion coefficient in the subdiffusive static case determines the Kubo number dependence of the asymptotic diffusion coefficient in a time-dependent potential. The subdiffusive transport corresponds to Lagrangian correlations $L(t)$ which have the property:

$$D(t) = \int_0^t L(t)dt \underset{t\to\infty}{\to} 0. \tag{40}$$

We suppose that $D(t)$ decays to zero as $D(t) \sim (t/\tau_{fl})^{-\alpha}$ and consequently the LVC behaves as $L(t) \approx -\alpha V^2 (t/\tau_{fl})^{-\alpha-1}$. In the time-dependent case, the variation of the stochastic field produces the decorrelation of the Lagrangian velocity and consequently the LVC is cut down at $t \gtrapprox \tau_c$. The asymptotic diffusion coefficient can be evaluated as the integral from 0 to τ_c of the LVC and using Eq. (40) one can write

$$D \simeq -\int_{\tau_c}^{\infty} L(t)dt = D_B K^{-\alpha} = \frac{\lambda_c^2}{\tau_c} K^{1-\alpha}, \tag{41}$$

which gives $\gamma = 1-\alpha$. Thus the exponent α of the time decay of the subdiffusive transport coefficient in the static case determines the exponent of the K dependence of the asymptotic diffusion coefficient in the time-dependent case. This means that Eq. (39) holds even if the evolution of $D^{td}(t)$ is not given by Eq. (38) as happens, for example, when the EC function of the potential is not factorized.

The time variation of the potential determines a decorrelation effect. After a time of the order τ_c the configuration of the stochastic potential changes. A competition appears between the intrinsic tendency of the trajectories to form structures and the destruction of these structures produced by the time variation of the potential field. Structures with $\tau_s(S) \gtrsim \tau_c$ cannot exist and the corresponding trajectories produce a diffusive transport. Small structures that build up rapidly (with $\tau_s(S) \ll \tau_c$) still exist if the correlation time of the field is longer than the flight time [$\tau_c > \tau_{fl}$, $K > 1$]. These vortical structures do not contribute to the large time values of the diffusion coefficient and the transport is reduced.

VII. CONCLUSIONS

We have studied the special problem of test particle transport (tracer advection) in two-dimensional divergence-free stochastic velocity fields, which is characterized by the intrinsic trapping of the trajectories on the contour lines of the stochastic potential. We have shown that the statistical behavior of the trapped trajectories is completely different from that of the free trajectories. The trapped trajectories have a quasicoherent behavior. The average, dispersion, and probability distribution function for these trajectories and for the distance between two trajectories saturate. A very strong anomalous clump effect characterizes neighboring trapped trajectories, which have clump lifetimes much longer than the time of flight. This shows that these trajectories form structures similar to fluid vortices. The statistical parameters of these structures (size, buildup time, dispersion) are determined. The trajectories contained in such structures do not contribute to the large time diffusion coefficient. The latter is determined by the free trajectories which have a continuously growing average displacement and dispersion. The probability distribution functions for both types of trajectories are non-Gaussian. Both types of trajectories are far from Gaussian and Markovian processes.

The Lagrangian velocity correlation and the time-dependent diffusion coefficient are determined as functionals of the Eulerian correlation of the stochastic potential. Long time algebraic tails are obtained for these functions, which determine a subdiffusive transport in a static potential and asymptotic diffusion coefficients with weak dependence on the Kubo number ($D \sim K^{\gamma}$ with $\gamma < 1$) for time-depending stochastic potentials.

We have developed a semianalytical statistical approach, the nested subensemble method, which is in agreement with all the statistical constraints imposed by the invariance of the potential in each realization. Essentially, this method reduces the problem of determining the statistical behavior of the stochastic trajectories to the calculation of weighted averages of some smooth, deterministic trajectories determined from the EC function of the stochastic potential. The one- and two-point Lagrangian statistics are determined here, but this approach can be extended to multipoint Lagrangian statistics, which were shown recently to be very relevant for the study of passive field advection [6–9].

The general conclusion of this work is that the existence of a Lagrangian invariant in the evolution equation (in each realization) determines long time correlations (memory effects) and coherence (trajectory structures) in the stochastic motion.

ACKNOWLEDGMENTS

This work was performed during our stay at National Institute for Fusion Science, Japan. We warmly acknowledge the hospitality of Professor M. Fujiwara and Professor O. Motojima. We want to thank Professor K. Itoh for very fruitful discussions and Professor R. Balescu and Dr. J. H. Misguich for their stimulating interest in this problem.

[1] W. D. McComb, *The Physics of Fluid Turbulence* (Clarendon, Oxford, 1990).
[2] J. P. Bouchaud and A. George, Phys. Rep. **195**, 128 (1990).
[3] A. S. Monin and A. M. Yaglom, *Statistical Fluid Mechanics: Mechanics of Turbulence* (MIT Press, Cambridge, MA, 1973), Vol. I.
[4] W. H. Matthaeus, G. Qin, J. W. Bieber, and G. P. Zank, Astrophys. J. Lett. **590**, L53 (2003).
[5] J. A. Krommes, Phys. Rep. **360**, 1 (2002).
[6] G. Falkovich, K. Gawedzki, and M. Vergassola, Rev. Mod. Phys. **73**, 913 (2001).
[7] A. Pumir, B. I. Shraiman, and M. Chertkov, Phys. Rev. Lett. **85**, 5324 (2000).
[8] I. Arad, L. Biferale, A. Celani, I. Procaccia, and M. Vergassola, Phys. Rev. Lett. **87**, 164502 (2001).
[9] G. Boffetta, A. Celani, S. Musacchio, and M. Vergassola, Phys. Rev. E **66**, 026304 (2002).
[10] R. H. Kraichnan, Phys. Fluids **19**, 22 (1970).
[11] S. Corrsin, in *Atmospheric Diffusion and Air Pollution*, edited by F. N. Frenkiel and P. A. Sheppard (Academic, New York, 1959).
[12] P. H. Roberts, J. Fluid Mech. **11**, 257 (1961).
[13] J. A. Krommes, in *Handbook of Plasma Physics*, edited by A. A. Galeev and R. N. Sudan (North-Holland, Amsterdam, 1984), Vol. 2, Chap. 5.5.
[14] J.-D. Reuss, M. Vlad, and J. H. Misguich, Phys. Lett. A **241**, 94 (1998).
[15] A. J. Majda and P. R. Kramer, Phys. Rep. **314**, 237 (1999).
[16] H. L. P'ecseli and J. Trulsen, J. Fluid Mech. **338**, 249 (1997).
[17] M. B. Isichenko, Plasma Phys. Controlled Fusion **33**, 809 (1991).
[18] M. Vlad, F. Spineanu, J. H. Misguich, and R. Balescu, Phys. Rev. E **58**, 7359 (1998).
[19] M. Vlad, F. Spineanu, Phys. Scr., T **107**, 204 (2004).
[20] J. P. Gleeson, Phys. Rev. E **66**, 038301 (2002).
[21] M. Vlad, F. Spineanu, J. H. Misguich, and R. Balescu, Phys. Rev. E **66**, 038302 (2002).
[22] G. I. Taylor, Proc. London Math. Soc. **20**, 196 (1921).
[23] T. H. Dupree, Phys. Fluids **10**, 1049 (1967).
[24] J. B. Taylor and B. McNamara, Phys. Fluids **14**, 1492 (1971).
[25] R. J. Adrian, Phys. Fluids **22**, 2065 (1979).
[26] J. R. Philip, Phys. Fluids **11**, 38 (1968).
[27] W. Feller, *An Introduction to Probability Theory and its Applications*, 2nd ed. (Wiley, New York, 1971), Vol. 2.
[28] M. Vlad, F. Spineanu, J. H. Misguich, J.-D. Reuss, R. Balescu, K. Itoh, and S.-I. Itoh, Plasma Phys. Controlled Fusion **46**, 1051 (2004).